Study Of Exchange Biasing Anisotropy In IrMn/Co Thin Films

A thesis submitted in partial fulfillment of the requirements for the degree of Bachelor of Science with Honors in Physics from the College of William and Mary in Virginia.

By

Haley Dawn Showman

Accepted for_____

(Honors, High Honors, or Highest Honors)

_____

Dr. Anne Reilly, Advisor

_____

Dr. Keith Griffioen

_____

Dr. David Armstrong

_____

Dr. David Stanford

Williamsburg, Virginia

April 2002

Abstract

This work explores exchange biasing in a bilayer thin film system consisting of the antiferromagnet IrMn and the ferromagnet Co. The exchange biasing interaction occurs at the interface between the antiferromagnet and ferromagnet, and results in a pinning of the ferromagnetic magnetization in a particular direction. The quantum mechanical Magneto-Optical Kerr Effect (MOKE) was used to measure the exchange bias field and coercivity of the films, which are studied as a function of Co layer thickness. This work shows that the exchange bias field and coercivity follow the behavior reported for other systems. Specifically, we observe that the exchange bias field is inversely proportional to the ferromagnetic layer thickness. This dependence has been formulated in several theoretical models. The results are analyzed and compared with the Malozemoff model of exchange biasing. We find that the exchange biasing energy is comparable to that of other IrMn systems and that our data fits well with Malozemoff's random roughness model.

Acknowledgements

I would like to express my gratitude to the many individuals who have helped, encouraged, and supported me in my academic undertakings in Physics. Thank you Dr. Reilly for all of your help and guidance in writing this thesis, taking data, and answering my millions of questions. I have truly enjoyed working with you this year. Thank you also for your patience and understanding in working around my crazy spring schedule! Thank you Hailong for the many hours that you have given of your own time to help me with the MOKE setup and tweek the system to get "pretty" hysteresis loops. You certainly went above and beyond the call of duty in helping me in the lab this year. Thank you Dr. Griffioen, Dr. Armstrong, and Dr. Stanford for taking the time to read my thesis and hear my defense. And finally, thank you Fiona, Catherine, Stephanie, and Dan for your unending support and encouragement as I pursued this degree and thesis work. I couldn't have made it this far with out you!

List of Figures

Page #

Table of Contents

I. Introduction

As engineers and computer manufacturers look for ways to make faster computers and data storage devices, scientists work to gain a physical understanding of the phenomena involved in such applications. Recently, scientists have given much attention to thin film technology. Thin films—on the order of 100-1000 Å in thickness—display some magnetic properties that cannot be found in bulk magnetic material and are utilized in a variety of applications including magnetic sensors and magnetic storage media. One topic of current interest is Giant Magnetoresistance (GMR), in which the resistivity of a material can be changed from relatively low to high by switching the direction of the magnetization of the material. An interest in GMR has led to renewed studies of some of the phenomena involved in magnetic thin films, including a shifting of the magnetic hysteresis loop due to the phenomenon of exchange biasing.

In 1956 Meiklejohn and Bean [1] discovered exchange biasing (EB), which occurs at the interface of antiferromagnetic (AFM) and ferromagnetic (FM) layered materials. In this effect, the magnetization of a ferromagnetic layer becomes "pinned" in a particular direction due to magnetic coupling with the surface of the antiferromagnet. As a result, the material is more easily magnetized in one direction than another, leading to a unidirectional anisotropy in the material. Exchange biasing received great attention about 10 years ago, when scientists found that EB was useful in applications involving GMR [2], such as magnetic sensors and stabilizers, and magnetic reading head devices. But scientists are still far from obtaining a clear theoretical understanding of the exchange bias interaction. Since the discovery of EB, many scientists have put forward theories to explain the phenomenon, but none have succeeded in describing the complete interaction in agreement with experimental results [2].

In this thesis work, the Magneto-Optical Kerr Effect (MOKE) is used to study exchange biasing in the IrMn/Co thin film system (where IrMn is the antiferromagnetic layer and Co is ferromagnetic layer) as a function of the ferromagnetic layer (Co) thickness. Experiments have shown [2, 3, 4] that for almost all AFM/FM systems, the exchange field is inversely proportional to the thickness of the ferromagnetic layer of a thin film. We will use the Magneto-Optical Kerr Effect to determine if this is true in a IrMn/Co system Although many AFM/FM systems have been studied, including the closely related IrMn/$Co_{90}Fe_{10}$ system [5], to our knowledge work on IrMn/Co has not been reported.

II. Theoretical Considerations

A. Ferromagnetism and Antiferromagnetism

The films we are studying consist of layers of ferromagnetic and antiferromagnetic materials. A ferromagnetic has a net spontaneous magnetic moment in the absence of an external magnetic field. In ferromagnetic metals, experiment shows that the magnetic moment due to the electron orbital angular momentum is negligible when compared with the moments due to the spin of the electron [6], thus the unpaired electrons can be thought of as little bar magnets, with the direction of their magnetic field defined by the direction of their spin.

Due to the Pauli exclusion principle, unpaired electrons with parallel spins will align themselves in orbits that tend to maximize the distance between them. The Pauli exclusion principle dictates that no two electrons can be in the same state at the same point in space and thus the wave functions of two electrons must be antisymmetric under the exchange of electrons [7] so that

$$\psi(r_1,s_1:r_2,s_2) = -\psi(r_2,s_2:r_1,s_1). \quad (1)$$

Thus, electrons of the same spin tend to stay far apart, which minimizes the Coulomb repulsion energy that is proportional to 1/r. The energy related to this exchange of electrons (named the exchange energy) can be written

$$E_{int} = -2J_{INT}\, \boldsymbol{S_i S_j} \cos \phi_{ij} \qquad (2)$$

Where S_i and S_j are the spins of the electrons, ϕ is the angle between the magnetic moments of the spins, and J_{INT} is an exchange parameter that is positive for ferromagnetic materials. We can see that the energy is minimized for positive J_{INT} when $\cos\phi_{ij} = 1$, or $\phi_{ij} = 0$ [6]. Although Equation (2) is written as a function of the spin orientation, its origin comes from the Coulomb interaction between the electrons (J_{INT} can be calculated from the Coulomb terms in the Hamiltonian).

This alignment of spins is affected by the thermal energy of a solid, which increases the movement of atoms and forces electron spins to become more randomly aligned. Above a critical temperature, known as the Curie temperature, the motion of the electrons overcomes the magnetic alignment, and the material ceases to show net magnetic properties. Some well-known ferromagnets, such as iron, have relatively high Curie temperatures (1043K for Fe, 1404K for Co and 627K for Ni), and so are magnetic at room temperature [7].

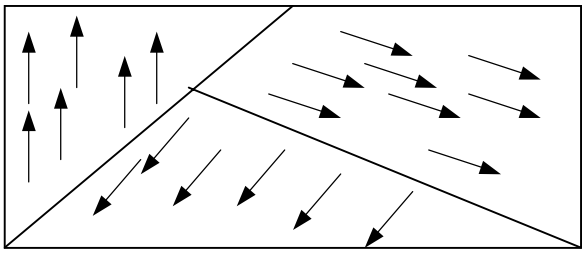

Figure 1: Electron spins aligned within domains in a ferromagnet

Ferromagnetic materials are made up of domains, or groups of 10^9 to 10^{15} atoms with all of the spins aligned in one direction (see Figure 1). This spin alignment occurs to minimize the

magnetic energy. A single magnetic domain would produce a large magnetic field (called the demagnetizing field) which would have energy associated with it. There is a net magnetization within a domain; however, the direction of one domain is different from that of its neighboring domains, so that the net magnetization in the bulk material, and thus the energy, is reduced. If a ferromagnet is placed in an external magnetic field H, the field exerts a force on the electron spins. Those domains that have a magnetization component parallel with the external field will grow by "stealing" a few electron magnetic moments from another domain that is not as favorably aligned. When the external magnetic field is strong enough, all the domains will combine into one, and the net magnetization will be forced in the direction of the applied field [6]. When the external field is removed, the electrons "remember" their preferred alignment—the majority stay aligned in the direction of the applied field and the material retains a net magnetic moment. A simple schematic diagram, similar to that described in Rudden and J. Wilson, is shown in Figure 2. With no external field (Figure 2a), the different domains are aligned in random directions, and the net magnetization for the solid is zero. When an external field is applied, domains 1 and 2 grow at the expense of domains 3 and 4, which do not have components in the direction of the applied filed (Figure 2b). Once the external field is strong enough, all of the domains combine, and align with the applied field (Figure 2c), and the sample has reached magnetic saturation—that is, the maximum possible magnetization for the sample. The external field is removed and only a few atoms return to their random alignment (Figure 2d), and the sample retains a net magnetic moment called the residual magnetization.

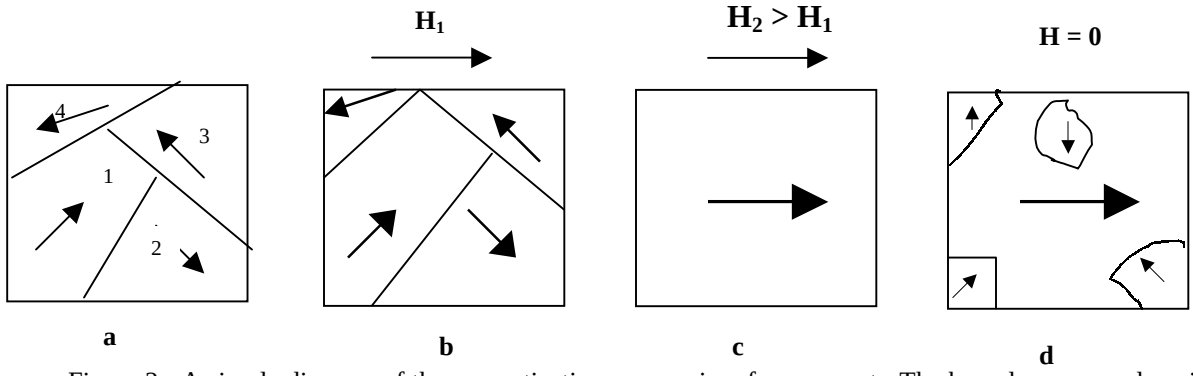

Figure 2: A simple diagram of the magnetization process in a ferromagnet. The bounds between domains are the domain walls, which disappear once the sample has reached saturation.

Because magnetic materials "remember" past configurations, a hysteresis loop is formed when the total magnetization (M) of a ferromagnet is plotted vs. the applied field (H). This hysteresis comes from the motion of the domain walls, or the transition layer between magnetic domains. As the applied field is increased, magnetic moments within the domain walls rotate and move such that the domains "grow" as shown in Figure 2a to 2d above. If an external field is applied in the opposite direction, the sample remains mostly magnetized in the original direction until a certain field strength is reached. Then, the domain action reverses and soon the process will repeat with the material being magnetized the direction of the new field, opposite to the original direction. When this field is then decreased back to zero, then the initial field applied, we complete the hysteresis loop as show in Figure 3. The half-width of a magnetic hysteresis loop is called the coercivity (H_C) of the material, and describes the strength of magnetic field required to flip the direction of magnetization in a certain sample. In Figure 3, the coercivity is given by

$$H_C = (p_1 - p_2)/2. \qquad (3)$$

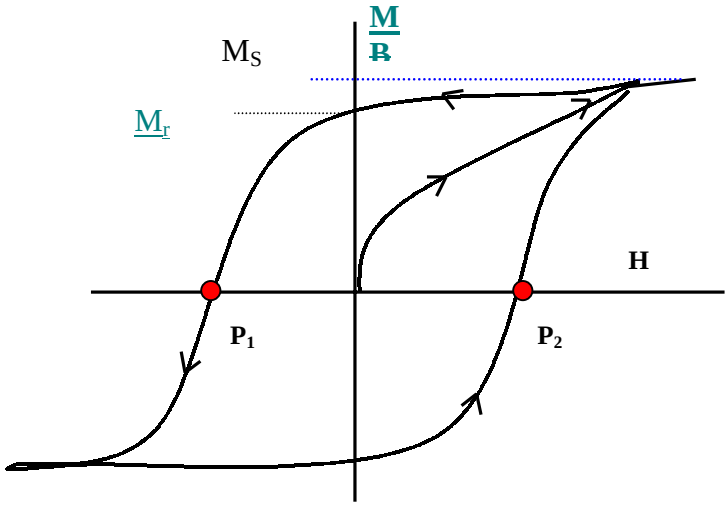

Figure 3: An example of a magnetic hysteresis loop. M is the magnetization of the sample and H is the applied magnetic field. M_S is the saturation magnetization and Mr is the residual magnetization.

Not all materials are ferromagnetic. Most bulk materials are either diamagnetic or paramagnetic, which means that they have no spontaneous magnetic moment. Another type of material is that in which the antiparallel alignment of electron spins is energetically favorable [7]. In this case, the crystal lattice of the material is divided into two equal sublattices A and B, and the spins of the electrons on A are antiparallel to those on B. Thus, the net magnetic moment over the entire lattice is zero. This material is called antiferromagnetic, and some examples are CoO, FeMn, IrMn [3] and NiO [4]. Like ferromagnets, antiferromagnets will loose their spin alignment above a certain temperature called the Néel temperature.

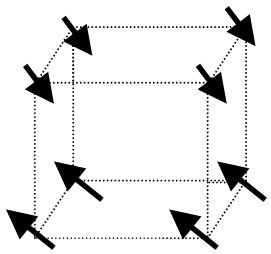

Figure 4: A simple diagram of one unit cell of an antiferromagnet. The arrows represent the electron spins for atoms in a simple cubic lattice structure.

B. Magneto-Optical Kerr Effect (MOKE)

Several methods exist for studying the magnetic properties of materials. Such methods include vibrating sample magnetometery (VSM), and SQUID magnetometery, where the magnetization (M) of the material is directly measured. Another method utilizes the Magneto-Optical Kerr Effect (MOKE) in order to study the hysteresis loops as a function of applied field. MOKE is a quantum mechanical effect that involves the rotation of the polarization of reflected light incident upon a material placed in a magnetic field. For paramagnetic materials, this effect is quite small, but for FM (ferromagnetic) materials, the Kerr effect causes rotations that are easily measurable [8]. Incoming polarized light incident on a magnetic film will be reflected with the polarization changed slightly from its original alignment. The change is directly proportional to the net magnetization of the material reflecting the light [8]. Although MOKE has the disadvantage of not giving a direct measurement of the absolute magnitude of the magnetization, it is very useful for measuring the shape of the hysteresis loop and the behavior of the magnetization as a function of applied field. MOKE is especially convenient when studying the direction dependant properties of a magnetic thin film, since a sample can easily be rotated (or even translated) with respect to the incident laser light beam. MOKE is also relatively straightforward to set up and is much less expensive than VSM and SQUID magnetrometry.

Three types of Kerr effects can occur, depending upon the alignment of the incident light and the magnetization of the sample. The polar Kerr effect involves magnetization components normal to the surface of the sample, and will not be dealt with in this thesis. The transverse and longitudinal Kerr effects occur when the external magnetic field is parallel to the face of the sample, as in Figure 5. The **p** and **s** directions are defined relative to the plane of light reflection, with **p** parallel to the plane of incidence, and **s** perpendicular to **p**. The transverse Kerr effect

describes magnetization perpendicular to the plane of incidence (the **s** direction), while the longitudinal Kerr effect involves magnetization parallel to the plane of incidence (the **p** direction). To measure MOKE, incident light is first passed through a polarizer, and reflected light is passed through an analyzing polarizer (analyzer).

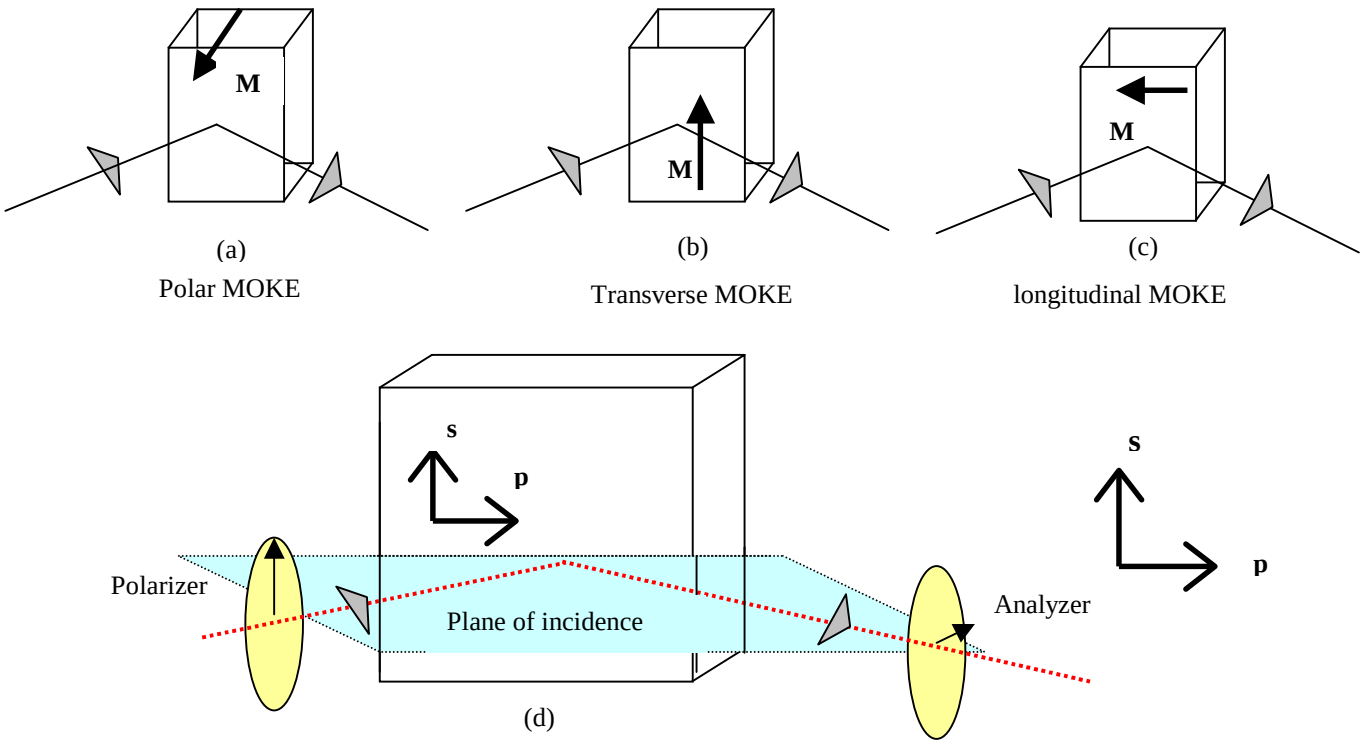

Figure 5: The different Kerr Effects. M is the magnetization of the sample, and the arrows represent the direction of the incident light.

When electromagnetic radiation is incident upon a surface, the ratio of reflected and incident wave intensities can be described using the Fresnel equations [9]. When light is incident on a ferromagnetic material, the reflection is affected by the magnetization of the sample, and this is reflected in the Fresnel coefficients. For the transverse Kerr effect, the Fresnel coefficients [10] are

$$r_{pp}^{t} = \left(\frac{n\beta - \beta'}{n\beta + \beta'} \right) \left(1 + \frac{\kappa_2 \sin 2\theta}{n^2 (n^2 \cos^2 \theta - 1) + \sin^2 \theta} \right), \qquad r_{ss}^{t} = \frac{\beta - n\beta'}{\beta + n\beta'}, \qquad r_{ps}^{t} = r_{sp}^{t} = 0 . \quad (4)$$

The longitudinal Kerr effect can be described with the longitudinal Fresnel reflection coefficients:

$$r_{pp}^{l} = \frac{n\beta - \beta'}{n\beta + \beta'} \ , \ r_{ss}^{l} = \frac{\beta - n\beta'}{\beta + n\beta'} \ , \qquad r_{ps}^{l} = -r_{sp}^{l} = \frac{\sin\theta \cos\theta \kappa_2}{n^2 \beta' (n\beta + \beta')(\beta + n\beta')} \quad (5)$$

where n is the index of refraction, θ is the angle of incidence from the sample normal,

$$\beta = \cos\theta, \quad \text{and} \quad \beta' = \sqrt{1 - \frac{\sin^2 \theta}{n^2}} . \quad (6)$$

The term κ_2 is the off diagonal element of the relative permittivity tensor, and

$$\kappa_2 = in^2 Q \quad (7)$$

The term Q is the Voigt magneto-optical parameter, which accounts for the quantum mechanical interaction of the magnetic electrons and the electromagnetic field, and is proportional to the magnetization in the ferromagnetic sample.

Fresnel coefficients make up the reflection matrices that describe the electric field of the reflected wave given by

$$E_{reflected} = \boldsymbol{S} E_{incident} \quad (8)$$

With the matrix

$$S = m_t^2 S^t + m_l^2 S^l \quad (9)$$

Where $m_t = M_t/M_s$ and $m_l = M_l/M_s$. $M_{t,s}$ are the components of magnetization parallel and perpendicular to the plane of incidence respectively, and M_s is the saturation magnetization. And the transverse and longitudinal matrices given by

$$S^t = \begin{pmatrix} r^t_{pp} & r^t_{ps} \\ r^t_{sp} & r^t_{ss} \end{pmatrix} \qquad S^l = \begin{pmatrix} r^l_{pp} & r^l_{ps} \\ r^l_{sp} & r^l_{ss} \end{pmatrix} \tag{10}$$

respectively. The terms r_{pp} and r_{ss} are the ordinary Fresnel reflection coefficients, while the off-diagonal terms r_{sp} and r_{ps} describe the change in polarization due to the magnetization of the surface. Here the notation $r^{t(l)}_{ab}$ refers to the transverse (longitudinal) effect on the reflected *a* wave by the incident *b* wave [10].

The off diagonal elements of the transverse matrix, r^t_{sp} and r^t_{ps} are zero, and thus there is no rotation of the polarization in the transverse Kerr effect. Rather, the magnetization of the sample only affects the amplitude of the **s** and **p** components of the reflected wave [10]. In contrast, the off diagonal elements for the longitudinal Kerr effect are dependent on the magnetization, resulting in a rotation of the polarized light that is proportional to the magnetization of the sample. In the limit that the magnetization goes to zero, or Q ==> 0, the Fresnel coefficients reduce to those of reflection off of non-magnetic metal.

The Kerr effect arises from the difference in absorption of left and right circularly polarized light by the ferromagnetic medium. Linearly polarized light can be broken down into equal quantities of right circularly polarized (rcp) and left circularly polarized (lcp) light [11]. Classically, MOKE can be described as arising from the different refractive indices for the lcp and rcp polarized modes in the dielectric tensor of a ferromagnetic material [12]. Quantum mechanically, the difference in the refractive indices can be explained in terms of the change in the wave functions arising from the spin-orbit interaction. The spin-orbit interaction is the bridge between the magnetic and optical properties of a ferromagnet, as it couples the electron motion to its magnetic moment [12]. Due to the spin-orbit interaction, the lcp and rcp light causes transitions between quantum states at different rates, and are absorbed differently[12].

The result is that the two circularly polarized modes gain different phase shifts, and that the ellipticity of the light changes [12] causing a rotation in the light polarization. The spin-orbit interaction is present in all materials, but only leads to a Kerr rotation in ferromagnetic materials because there is an unequal number of up- and down- electron spins (in non-ferromagnets, there are an equal amount of up and down spins and the effect is canceled).

The actual longitudinal and transverse Kerr effects described above can be measured by passing the incident light thorough an initial polarizer, then the reflected light through another polarizer analyzer. An incident polarized beam can be expressed [10] in the form

$$E_i = E_0 \cos\theta_p \mathbf{p} + E_0 \sin\theta_p \mathbf{s} \tag{11}$$

where θ_p is the angle of the polarizer (from **p**).

Applying Equation 11, the reflected amplitude is given by

$$\begin{pmatrix} E_p^{ref} \\ E_s^{ref} \end{pmatrix} = m_t^2 \begin{pmatrix} r_{pp}^t & r_{ps}^t \\ r_{sp}^t & r_{ss}^t \end{pmatrix} \begin{pmatrix} E_0 \cos\theta_p \\ E_0 \sin\theta_p \end{pmatrix} + m_l^2 \begin{pmatrix} r_{pp}^l & r_{ps}^l \\ r_{sp}^l & r_{ss}^l \end{pmatrix} \begin{pmatrix} E_0 \cos\theta_p \\ E_0 \sin\theta_p \end{pmatrix} \tag{12}$$

Taking into account that $r_{sp}^{\ t} = r_{ps}^{\ t} = 0$, $r_{ss}^{\ t} = r_{ss}^{\ l}$, and $m_t^2 + m_l^2 = 1$, Equation 12 reduces to

$$E_p^{ref} = (m_t^2 r^t_{pp} + m_l^2 r^l_{pp}) E_0 \cos\theta_p + m^2_l r^l_{ps} E_0 \sin\theta_p,$$

$$E_s^{ref} = m^2_l r^l_{sp} E_0 \cos\theta_p + r^l_{ss} E_0 \sin\theta_p \ . \tag{13}$$

In the experimental setup, it is convenient to fix the polarizer at 90º, or **s**-polarized, so that $\theta_p = 90^o$. Then Equation 13 reduces even further to

$$E_p^{ref} = m^2_l r^l_{ps} E_0,$$

$$E_s^{ref} = r^l_{ss} E_0 \ . \tag{14}$$

The field that is transmitted through the analyzer set at an angle θ_a is

$$E_t = E_s^{ref} \sin\theta_a + E_p^{ref} \cos\theta_a \ . \tag{15}$$

If the analyzer is set at a very small angle θ_a = 0º or 1º, then the transmitted intensity is approximately equal to the parallel component

$$E_t \approx E_p^{ref} = m^2{}_l r^l{}_{ps} E_0 \ . \tag{16}$$

This light can be detected via a photodiode whose output current from sensing the light is proportional to the square of the modulus of E_t (Equation 16).

$$\frac{I}{I_0} \propto \frac{|E_t|^2}{|E_0|^2} \propto \frac{|E_p^{ref}|^2}{|E_0|^2} = |m_l^2 r_{ps}^l|^2 \tag{17}$$

where

$$r_{ps}^l = \frac{\sin\theta\cos\theta\kappa_2}{n^2\beta'(n\beta+\beta')(\beta+n\beta')} \tag{18}$$

so that

$$\frac{I}{I_0} \propto \frac{M_l^4}{M_x^4} \frac{\sin^2\theta\cos^2\theta n^4 Q^2}{n^4\beta'^2(n\beta+\beta')^2(\beta+n\beta')^2} \ . \tag{19}$$

The intensity of light detected is dependent on the magnetization, and is also dependent on the incident angle θ.

C. Exchange Biasing

Exchange biasing (EB) is defined by a shift in the center of the magnetic hysteresis loop. EB occurs at the interface of various systems of Ferromagnetic/Antiferromagnetic (FM/AF) materials, including the interface of FM/AF thin films. The antiferromagnetic (AF) layer can cause the neighboring ferromagnetic (FM) layer to be “pinned” in a preferred direction of magnetization [13]. This anisotropy, or loss of directional symmetry, causes the center of the

hysteresis loop to shift to a position $H_E \neq 0$ called the exchange field. A change in the coercivity of the material also results from EB.

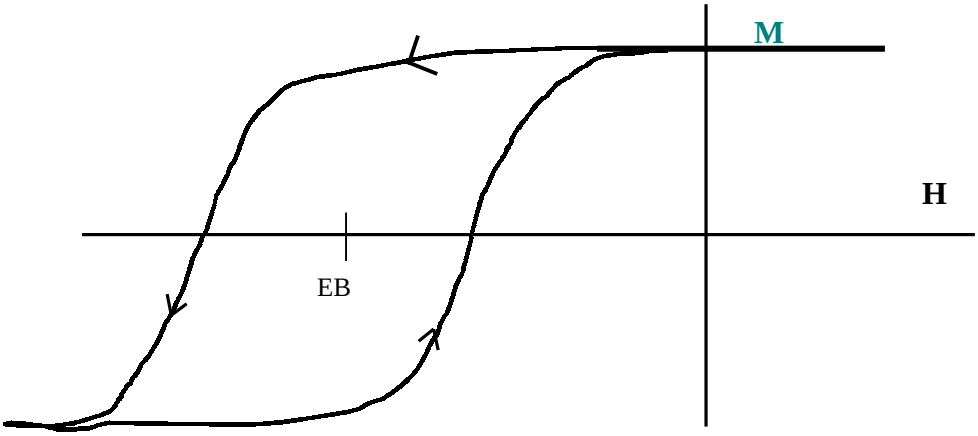

Figure 6: Hysteresis loop for an Exchange Biased sample. The center of the loop is the EB field. In most samples, the EB is negative, as shown.

To create an exchange-biased material, a sample must be "pinned" in one direction. Pinning is achieved by heating the material close to the Néel temperature, but not as high as the Curie temperature, then cooling in the presence of an external magnetic field [13].

A simple intuitive example of the pinning process can be explained as follows. Heating the film above the Néel temperature causes the electron spins in the AF to resume random alignment. An external field can then be applied which will cause the FM spins to align with the external field, while the AF spins remain randomly aligned. If the sample is then cooled below the Néel temperature in the magnetic field, the AF spins at the interface will align ferromagnetically with their neighboring FM electrons, and the other AF spins will fall into antiferromagnetic alignment accordingly, as in Figure 7. In many real applications, the pinning is set by raising the temperature to a value below the actual Néel temperature (this is called the blocking temperature, and it is the temperature above which the EB field would go to zero). The AF layer will remain pinned in this direction, causing the FM layer to "prefer" the pinned direction over any other. The interface AF spins will exert a small torque on the FM interface

spins, so that a significantly larger field will be required to magnetize the sample in the direction opposite to the pinning field. This creates a negative shift in the hysteresis loop relative to the pinning field direction.

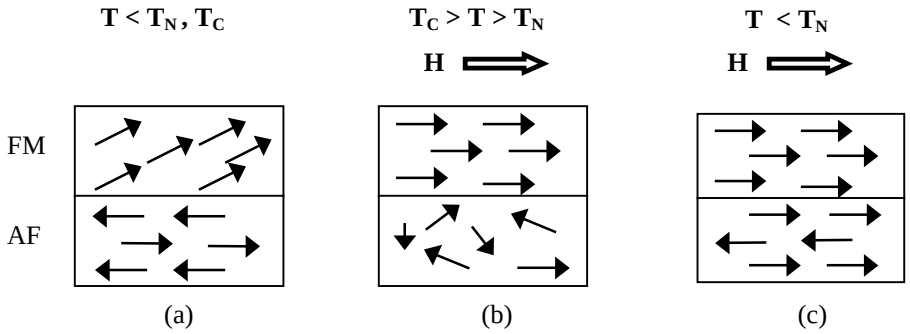

Figure 7: A simple picture of the pinning process. At (a) the sample is not in an external field, and is at a temperature below the Néel and Currie temperatures, T_N and T_C. The sample is then placed in an external field, H (b), then cooled below T_N (c) to pin the FM layer in the direction of the applied field.

Here, the pinned sample is an example of a *collinear* system since the FM and AF layers are magnetized in parallel planes. Early models of EB assume collinear FM/AF interfaces. More complicated EB systems can have noncollinear interfaces, with the FM spins at some angle $\theta \neq 0$ with the AF spins. Later EB models have accounted for such systems.

Since its discovery in 1956, scientists have been studying exchange-biased systems, but much work must still be done before a clear theoretical understanding of EB is reached [2]. Many models have been put forward to explain EB, but none have successfully matched all experimental results. Kiwi summarized several results, and concluded that "there are many systems that exhibit EB and it is quite likely that no single theory will be able to properly fit and describe all of them [2]." Unfortunately, the system that is most relevant for technological applications, the polycrystalline thin film, is also a system that is more difficult to explain by theory [2].

Among the most prominent factors affecting exchange biasing is the thickness of the magnetic layers in the thin films. Experiments have shown that the exchange field H_E drops abruptly as the thickness of the antiferromagnetic layer decreases below a critical thickness, and eventually vanishes for AF layers of only a few nm in thickness [3, 14, 15, 16]. For increasing thickness above the critical point, two different cases have been observed: the EB remains constant as a function of the AFM layer thickness, or the EB reaches a maximum and then continuously decreases.

The thickness of the ferromagnetic layer also has an affect on the EB. The earliest models for EB predict a linear dependence of H_E on the inverse of the ferromagnetic thickness [2,3]

$$H_E \propto \frac{1}{t_{FM}} \tag{20}$$

This basic dependence has been observed for all the systems studied [3]. Examples include the work by Mauri *et. al*, who found that an MnFe/NiFe system showed proportionality to the inverse of the FM thickness over a range of 50 to 400 Å [17]. Similar results were also reported by Tang *et. al*, who found a dependence of the coercivity on the inverse FM layer thickness [18]. The increase in coercivity is another common experimental result, though it has received less attention than the exchange field [3].

The basic thickness dependence can be seen in the original model by Meiklejohn [3]. Here, the energy per unit area of an EB system can be written [3] as

$$E = -HM_{FM}t_{FM}\cos(\theta-\beta) + K_{FM}t_{FM}\sin^2(\beta) + K_{AF}t_{AF}\sin^2(\alpha) - J_{INT}\cos(\beta-\alpha) \tag{21}$$

Here, H is the applied field, M_{FM}, the saturation magnetization, t_{FM}, and t_{AF} the thicknesses of the FM and AF films respectively. K_{FM} and K_{AF} are the anisotropies of the two layers, and J_{INT} is

the interface coupling constant. The three angles $\alpha, \beta, \theta,$ describe the angles between the anisotropy axis (assumed to be the same for K_{FM} and K_{AF} for collinear systems) and the magnetization of the two layers, and the applied field, as shown in Figure 8.

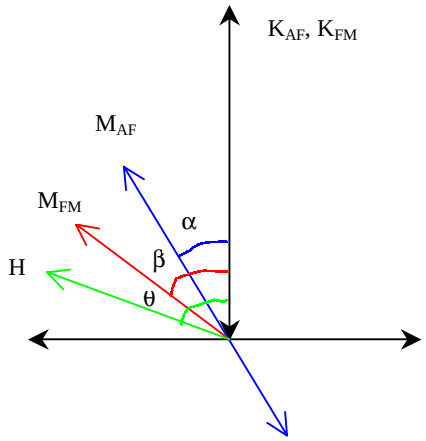

Figure 8: Diagram of the angles involved in the exchange bias system. After Nogues [3].

The energy of the exchange system as shown in Equation 21 is due to four factors, as can be seen in the four terms above. The first comes from the effect of the applied magnetic field on the FM, the second and third terms are due to the anisotropy of the FM and AF respectively, and the last term arises from the interface coupling. The simplest case (and what is often seen experimentally) assumes that the FM anisotropy is negligible, and thus the equation becomes:

$$E = -HM_{FM}t_{FM}\cos(\theta-\beta) + K_{AF}t_{AF}\sin^2(\alpha) - J_{INT}\cos(\beta-\alpha) \qquad (22)$$

If the energy is minimized with respect to α and β, the exchange bias field can be found [3]:

$$H_E = \frac{J_{INT}}{M_{FM}t_{FM}} \qquad (23)$$

The EB shift is dependant upon the value of J_{INT}, which was originally assumed to be similar to the ferromagnetic exchange. This early assumption resulted in calculated values of H_E several

orders of magnitude larger than experimental results [2,3]. This model does not account for many different parameters that come into play in EB systems—both intrinsic and extrinsic. The domain size in the AF and FM layers, domain behavior in the system, and interface roughness, are just a few of the factors that can be taken into account for different systems.

As more experimental data are taken, and more precise measurement techniques are developed, new models are presented to take these various parameters into account, and which give results closer to those found in the lab [2,3]. One example is a model presented in the 1980s in which A. P. Malozemoff considers both domain formation and a reduction in the exchange field due to formation of planar domain walls at the interface of the FM/AF with unfavorable ferromagnetic orientation [4]. This would reduce the exchange energy by a factor of the AF domain wall energy $4\sqrt{\frac{J_{AF}K_{AF}}{a}}$ thus modifying Equation 23 to:

$$H_E = \frac{2}{M_{FM}t_{FM}}\sqrt{\frac{J_{AF}K_{AF}}{a}} \quad . \tag{24}$$

where J_{AF}, K_{AF} and a are the exchange energy, anisotropy constant and lattice constant of the anitferromagnet. While this model yields a calculated exchange field much closer to that of experimental data, it remains larger than most measured exchange fields [4]. The exchange bias models given in Equations 23 and 24 both assume a perfectly smooth interface surface between the ferromagnetic and antiferromagnetic layers. In reality, the surface most likely contains small (atomic sized) defects that could cause a few electron spins to align in an random directions[4], as shown in Figure 9.

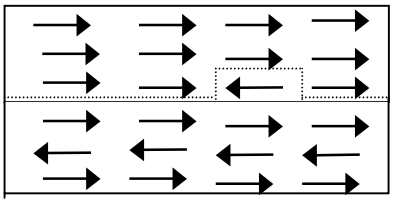

Figure 9: A possible random defect at the FM/AF interface. The dashed line represents the interface between the two materials.

Malozemoff postulates a randomness in the EB arising from interface roughness, which changes the effective exchange integral. At the site of interface roughness, planar domain walls may form at the interface of the roughness, and this will reduce the exchange energy to give

$$H_E = \frac{2z}{\pi^2 M_F t_F}\sqrt{\frac{J_{AF}K_{AF}}{a}} \qquad \textbf{(25)}$$

where z is a number of order unity. This model gives reasonable predictions for the exchange field [4].

III. Experimental Setup

A. The MOKE System

We exploit the Magneto-Optical Kerr Effect to study the magnetic properties of thin films. A MOKE system and Labview program are used to measure the magnetization of a sample verses the applied magnetic field. Hysteresis loops were taken, and the coercivity and exchange field were measured from this data. The experimental setup is shown below in Figure 10.

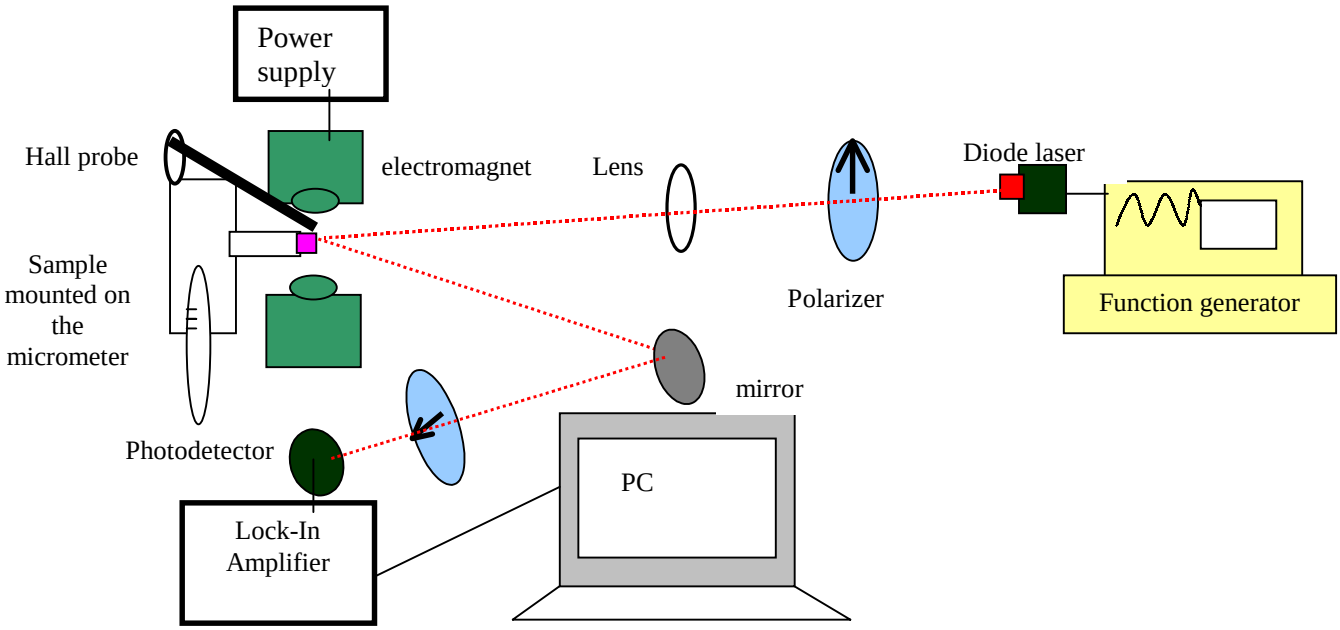

Figure 10: Our MOKE setup. This includes a diode laser, connected to a function generator, and set to a frequency of 100 KHz. This light beams passes through a polarizer set at an angle θ_1, then through a lens which focuses the beam before it hits the magnetic sample. The reflected light hits a mirror, then is sent through a second polarizer set at an angle near extinction with respect to θ_1. The resulting signal then enters a photodetector, where it is converted into an electric current and read in the lock-in Amplifier, which is set to read signals of 100 KHz. This data is sent to a PC where it is read in a Labview program, along with readings from the Hall probe, which detect the strength of the external magnetic field, produced by the electromagnet.

The MOKE experimental setup includes a Coherent Inc. diode laser source of monochromatic light (at 632 nm), two Glan-Thompson cube polarizers, a Stanford Research Systems function generator, lenses, and a GMW Inc. electro-magnet powered by a Kepco bipolar

power supply to create our external magnetic field **H**. A Hall probe mounted on a rod was placed in between the electromagnet poles to measure the magnetic field. The polarized laser light is incident on the sample in the magnetic field, as shown in Figure 10. The reflected light is detected by a Thorlabs silicon photodiode. A second analyzer polarizer aligned perpendicular to the first one will detect any change in polarization in the reflected beam. The extinction ratio of the two crossed polarizers is near 10^{-6}. A function generator modulates the diode laser beam and a Stanford Research Systems lock-in amplifier detects the signal from the photodiode. The shift in polarization is very small in MOKE (much less than a degree), and the lock-in technique allows detection of very small signals.

B. **Samples**

Dr. William Egelhoff of the National Institute of Standards in Maryland provided the exchange-biased samples for our studies. The first sample studied consists of Si(100)/thermal oxide/100Å Ta/100 $Ir_{20}Mn_{80}$/10-110Å Co wedge/12Å Al_2O_3, grown by sputtering. The second sample used was identical to the first, except it was subjected to a proper temperature for pinning (see below). The third sample used is of the same structure, except the cobalt wedge ranges in thickness from 10 Å to 170 Å. The AFM layer is a constant thickness, and is covered with the Co FM wedge of linearly varying thickness as shown below. The pinning in the second sample was set by heating the film in vacuum to 200°C and cooling back to room temperature in the presence of a 100 Oe field, while the third sample was heated to 250°C in otherwise the same conditions.

IrMn is an fcc structure, with a Néel temperature of 417^0C. The blocking temperature of IrMn is in the range of 200-250^{o}C. Co is an fcc or hcp structure. It prefers hcp, but grows fcc if

the layers below it are fcc. At a critical thickness, the Co will revert back to hcp structure. The Curie temp. of Co is 1131 ^{0}C.

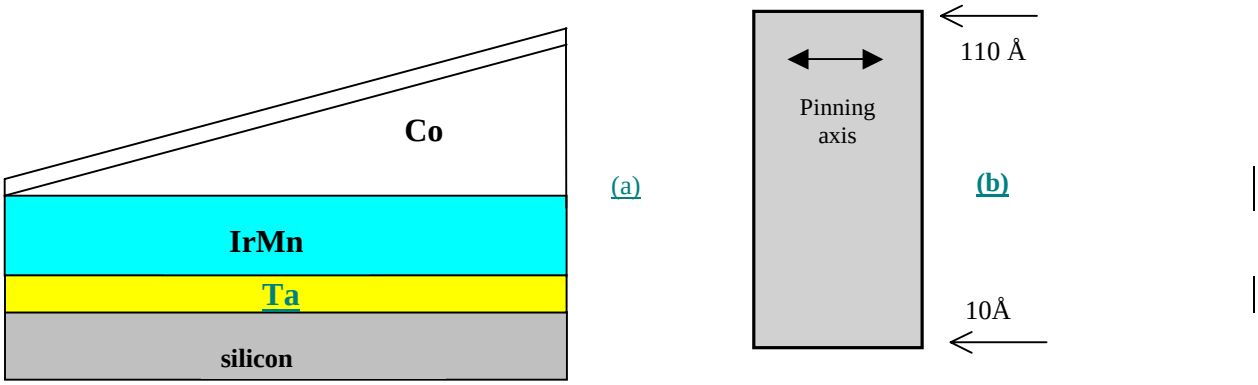

Figure 11: Diagrams of our Co/IrMn sample from the side (a) and top (b). The top layer is a protective coating of Al_2O_3, and the middle Ta layer helps the growth of the proper <111> orientation of the IrMn. The pinning axis is the axis of the EB field, ie: the cooling field.

The thickness of the Co increases linearly along the long axis. Thus the thickness can be related to the position along the sample by, for example for the first and second samples:

$$t_x = 110Å - 4x \tag{26}$$

where t is the thickness in Å and x is the distance in mm from the thick end of the sample.

For the third sample,

$$t_x = 170\ Å - 5.33x\ . \tag{27}$$

C. The Sample Mount

In order to accurately measure our wedged, multi-layered sample, we mount the sample on a double micrometer mount to allow for easy translation in both horizontal and vertical directions. Because the sample is wedged at a known, uniform slope, knowing the position of the laser beam on the sample is sufficient to determine the thickness of the FM layer being measured. The

micrometer mount allows us to raise and lower the sample, rather than change the position of the laser, which would involve changing the positions of the polarizers and lens.

IV. Preliminary Work

In order to ensure that our MOKE setup was working properly, we ran several tests on single layer FM thin films. The MOKE data for a normal FM film should result in a hysteresis loop with no exchange field, that is, the hysteresis should be centered on 0 Oe. The coercivity of each FM film should also remain constant with translation of the sample. We tested the MOKE system with samples of CoFe, Co, and NiFe thin films. After putting together the horizontal micrometer mount, we ran tests on the CoFe sample and took several hysteresis loops along the horizontal axis of our sample to determine if the coercivity changed as the sample was moved along the micrometer slide. The results are shown in Figure 12.

To compare the data from run to run and sample to sample, the data are all normalized along the y axis to + 1 and –1. This axis is a measure of the intensity of light hitting the photodiode. From the normalized plots, the shift in the hysteresis loop along the x axis (field) and the coercivity are determined. From the data given above, we can determine the error in our setup due to horizontal translation of the sample. We found that the hysteresis loops were shifted slightly from center, and the coercivity varied slightly with position, yielding a standard deviation of about 1.55 Oe.

Other parameters that must be taken into account include the position of the Hall probe inside the magnetic field, as well as the distance between the two poles of the magnet. Both will affect the field read by the Hall probe, and the pole separation will affect the field felt by the sample.

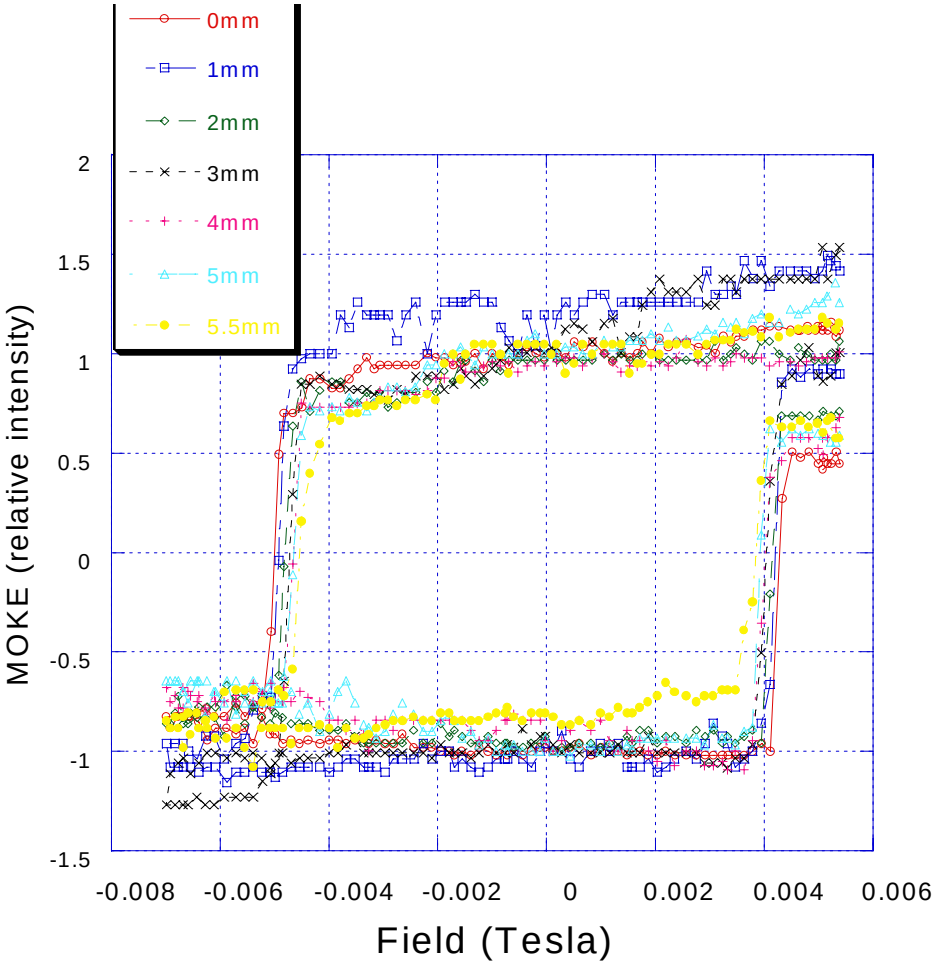

Figure 12: Plot of magnetization verses applied magnetic field for a sample of CoFe. The different colors of hysteresis loops represent different points along the length of the sample. The magnetization of the sample has been normalized into dimensionless units, and the applied field is given in Tesla (1 T = 10^4 Oe). The mm measurements refer to the laser position along the horizontal axis of our sample where 0mm refers to one edge of the sample.

The GMW magnet produces magnetic fields by running current through two large coils separated by a few centimeters. Within the coils are tapered iron poles to enhance and concentrate the field. The two poles can be moved with respect to one another. The closer the two poles are, the stronger and more uniform the field inside.

The Hall probe utilizes the Hall effect to measure magnetic field strengths. The magnetic field produced between these coils is not completely uniform along this axis, nor is the field uniform outside of the region between the coils. Figure 13 gives a simple diagram of the

magnet. Tests were run to determine the fluctuation in the Hall probe measurements along the x and y axis (parallel to and perpendicular to the two coils). The results are shown in Figure 14.

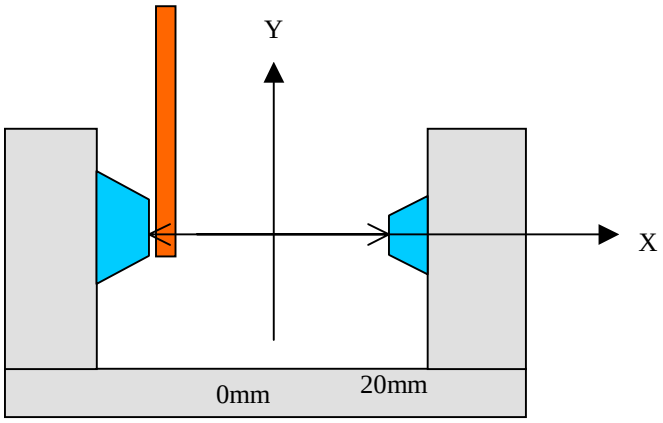

Figure 13: A diagram of the GMW electro-magnet and Hall probe (rectangle). The x-axis represents the line passing between the two coils, which are shown in blue. The Y-axis is vertical and perpendicular to the x-axis, as shown. Here, the total distance between the poles is 40mm.

The magnetic field fluctuations along the x and y-axis were measured and plotted below. As can be seen, deviations greater than 10 mm in the x or y direction can lead to significant changes in the magnetic field. Thus, it was critical to know the placement of the Hall probe relative to the sample. The position of the Hall probe then is critical in determining the exact field strength of the applied external magnetic sample. Fortunately, the dependence of the true field at the sample position versus the position where the Hall probe was placed is very linear in the x direction (Figure 14 c), thus a simple linear equation can be used to calculate the magnetic field at the sample. This equation, determined for the final sample run, was

$$H_{sample} = -2.29+0.691(H_{measured}). \quad \textbf{(28)}$$

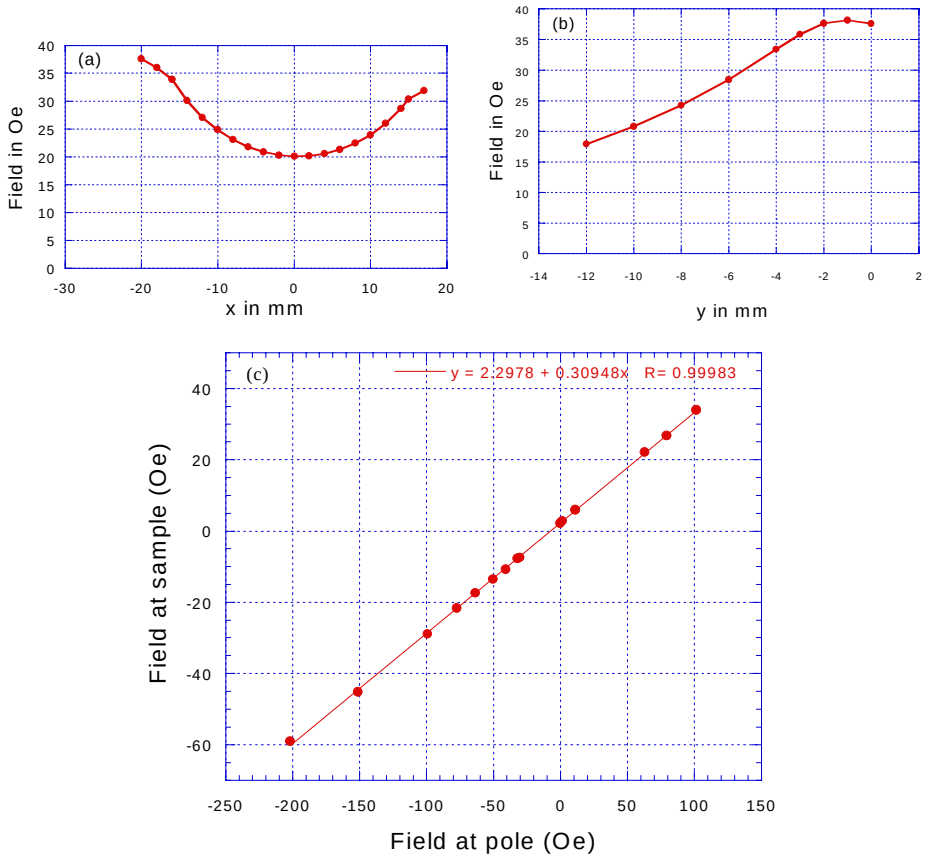

Figure 14: (a), (b) Hall probe readings as a function of the distance along the x and y-axis of the magnet. Here, zero is taken to be the center of the x-axis, exactly half way between the two coils, and in line with the center of the two coils. (c) The field felt by the sample in the middle of the magnet verses the field read by the Hall probe at one end of the magnet. The linear fit serves as a correction to the MOKE data.

V. Experimental Results

After configuring our MOKE setup with the plastic mount, we replaced the CoFe sample with our first Co/IrMn sample. We again took several measurements along the length of the sample to detect any dependence of the EB on the thickness of the Co layer. Three of our results are shown in Figure 15.

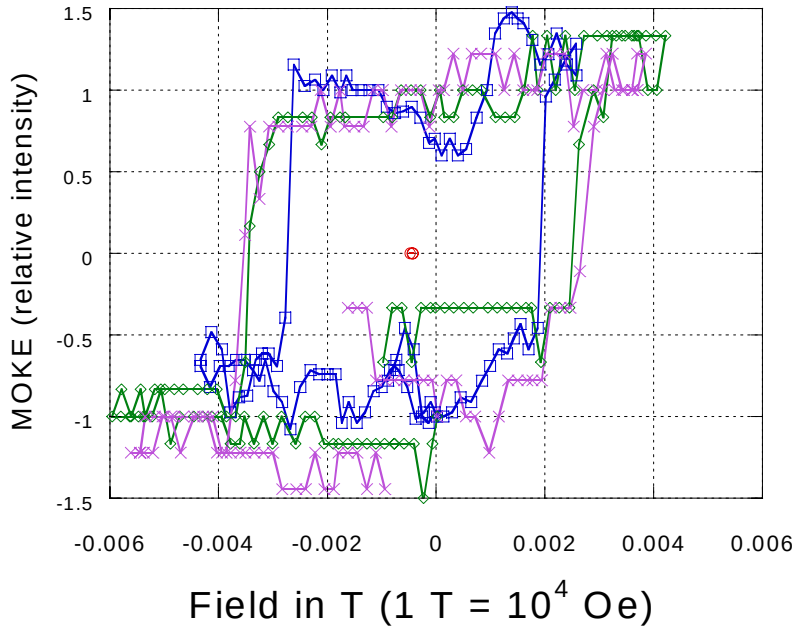

Figure 15: Magnetization verses applied field for varying thickness of the FM layer in IrMn/Co. The x-axis is the field in Tesla, and the y-axis is the MOKE intensity. The centers of the loops are plotted as points. Data were taken for Co layer thicknesses of about 110Å near the thickest part of the sample, and also at points near the center, where the Co layer is around 50Å.

Here, the hysteresis loops seem shifted slightly off center, but not as much as expected for an exchange-biased system. This most likely means that the sample was not properly "pinned" (we were informed by Dr. Egelhoff that the heater in the growth chamber was not working, which would greatly affect the pinning process as explained in the theory section).

Dr. Egelhoff provided another Co/IrMn sample similar to the first one. This second sample was heated to 200°C (with the heater working) and cooled in 100 Oe. The dimensions of the layers of this sample are identical to those of the first sample described above (Figure 10). The pinning is set along the short axis as in Figure 10, so that the sample was placed vertically in the magnetic field. The gradient was still along the long axis, so we added the vertical micrometer to the mount and moved the sample up and down to obtain data for varying Co thicknesses. We took several measurements with the MOKE system, beginning with the thick end (110Å of Co) of the sample and working down to the middle of the film. Our results showed that the film was

definitely exchanged biased, and that the EB depended on the thickness of the Co layer. Some of our results are shown below.

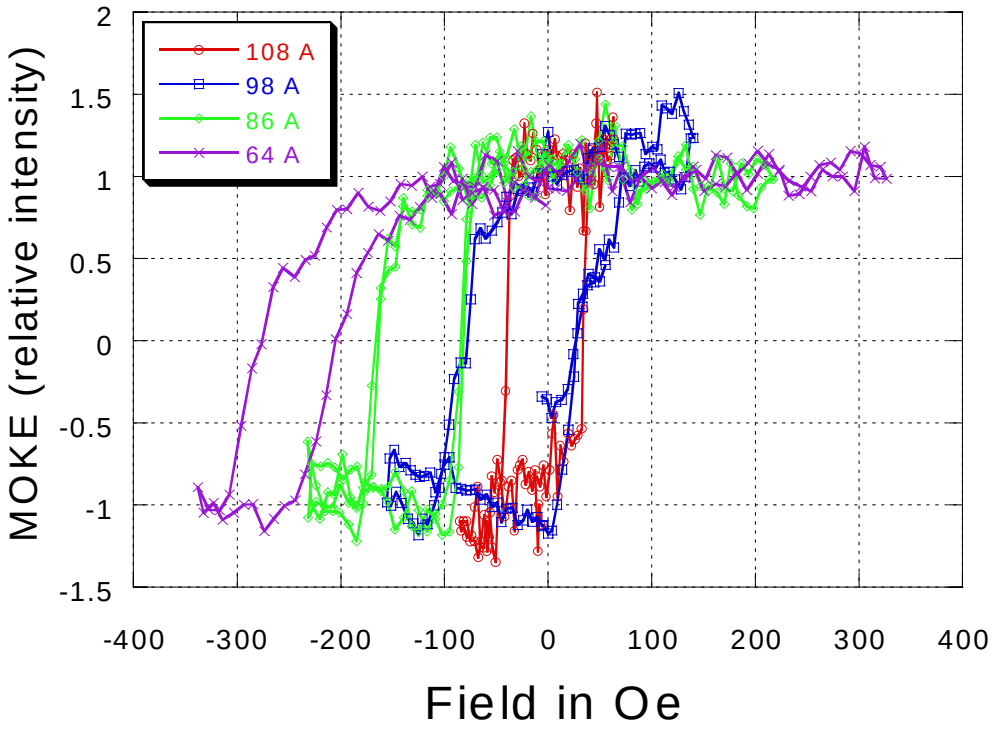

Figure 16: Magnetization verses applied field for varying thickness of the FM layer in Co/IrMn. The EB shift is obvious for thicknesses less than 108 Å. There is also a change in coercivity, or width of the hysteresis loop for the varying thicknesses.

The exchange bias field increases as the thickness of the Co layer decreases. This is in agreement with work done on other FM/AF bilayers such as NiFe/MnPd bilayers, which showed that the coercivity was linearly dependant on the inverse of the FM thickness [18]. We measured the thickness and coercivity for several different thicknesses along the sample, and plotted the results to determine the linearity of the thickness dependence.

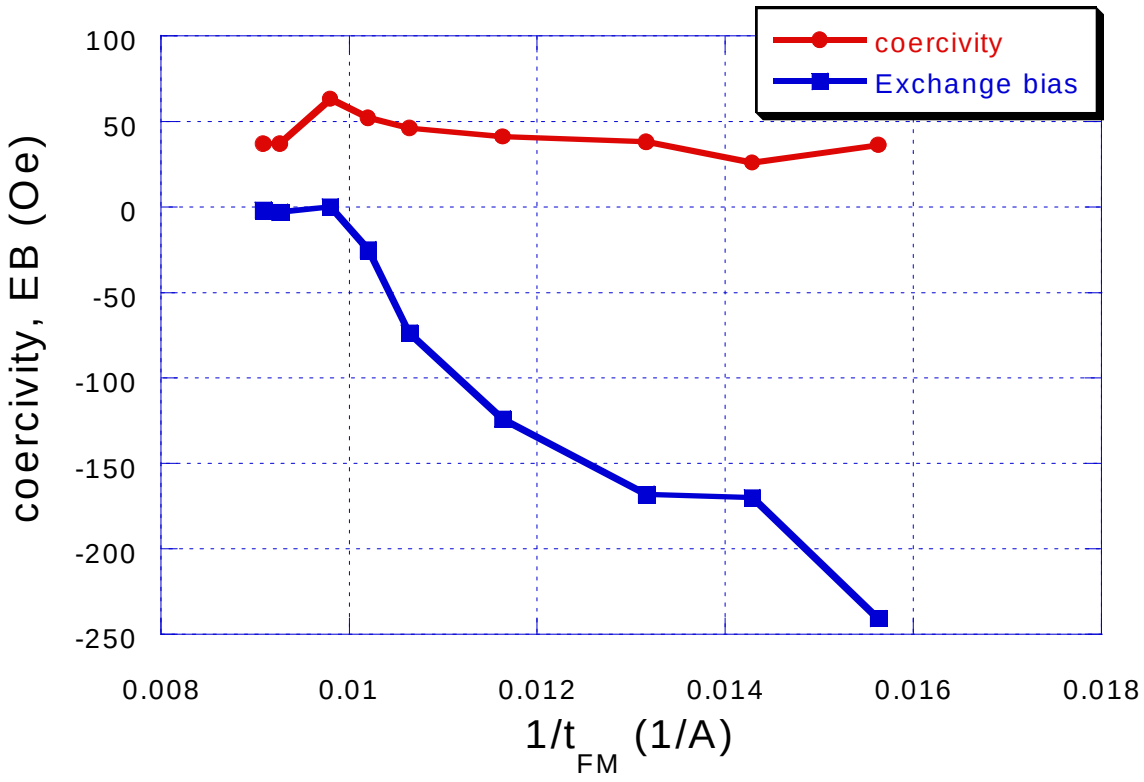

Figure 17: The results of MOKE data on the old, non-micrometer mount. The exchange field and coercivity definitely depend on the thickness of the FM; however, it is unclear if this dependence is linear. Fluctuations in the measurements are probably due to human error in position easements as well as movement of the sample caused by the strong applied field. The connecting lines are guides to the eye.

The exchange bias does indeed increase with decreasing thickness (fig 10). Since the measurement of the position of the laser on the sample was made by eye, an error of +/- 2Å can be accounted by the fact that the position could only be measured with in the nearest ½ mm. Also, the measurements of the CoFe sample showed fluctuations in the coercivity of about 2 Oe.

To eliminate some of the errors involved in the measurements, a new mount was made for the sample. The film was placed in a secure holder, and mounted on a vertical micrometer that allowed more accurate readings of the laser position along the sample. The same measurements were made on the sample with the new mount with the following results.

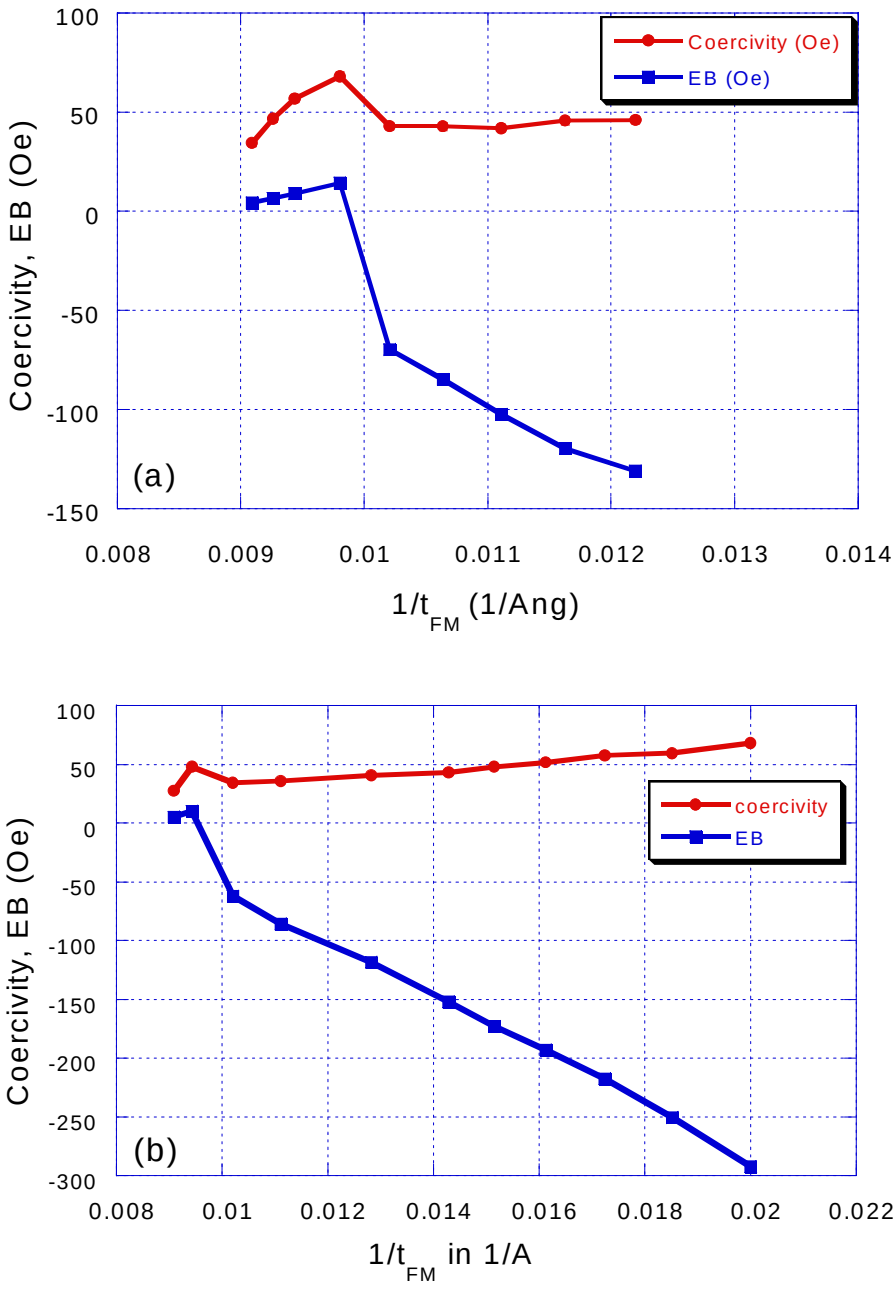

Figure 18: Results of measurements taken in two different runs on the secure micrometer mount. The exchange bias and coercivity both show linear behavior for thicknesses less than 100Å. Fig 18 (a) shows more data points for the thick end of the sample, emphasizing the unaccounted for behavior at thicknesses near 100Å. Fig. 18 (b) displays more data for the thinner end of the sample. A systematic error of +/- 4 Å occurs in the thickness measurement. The error is determined by the 0.01 mm resolution of the micrometer, which corresponds to 0.1 % of the smallest measured thickness. These error bars are smaller than the size of the data markers, and so can not be seen in the plot. A small field error of 2 Oe also arises due to the movement of the sample with in the magnetic field (See discussion with Figure 12). The connecting lines are guides to the eye.

The measurements at the thick end of the sample (1/thickness < 0.01) reveal interesting behavior for the Co/IrMn system. This may be attributed to the change in structure of the film of polycrystalline Co. It has been shown that thin layers of Co tend to have an fcc structure, whereas hcp structure will mix into the layer above a certain thickness (about 60Å). [19] The unaccounted for behavior could also arise from an uneven heating of the sample during the pinning process. The sample edges are held by clips that could interfere with the conduction of the heat during the pinning process, that would in turn affect the exchange field. To see if the strange behavior at 100 Å was due to this part of the sample being near the edge, a third sample was acquired in which the thickness varied from 10-170 Å, and thus the 100 Å region is near the middle of the sample.

Due to the necessary sharing of lab equipment, the magnet poles and Hall probe were both moved from their original position before correction measurements of the field accuracy, or the distance between the poles could be taken. The given values for the applied field, and thus the exchange and coercivity, are possibly offset from the actual value of the applied field at the position of the sample. For later results, these corrections are determined and taken into account.

The results show a definite linear dependence of both the exchange biasing and the coercivity on the inverse thickness. The non-uniformity of the earlier results are likely due to movement of the sample during the duration of the data runs due to the attraction of the magnetic film to the electro magnet. The new mount proved more stable and allowed for easy vertical translation of the sample.

The third sample was also tested using the micrometer mount. Hysteresis loops were taken for Co thicknesses ranging from 79.3 Å to 170 Å. The magnet poles were placed about 4cm apart, and thus the magnetic field fluctuated from the pole to the middle of the magnetic field.

These fluctuations, given in the previous section are taken into account, and the data was corrected by accounting for the difference in field from where it was measured compared to the sample position. The largest EB field measured was reduced from 157 Oe to 110 Oe. The corrected data is shown in Figure 19.

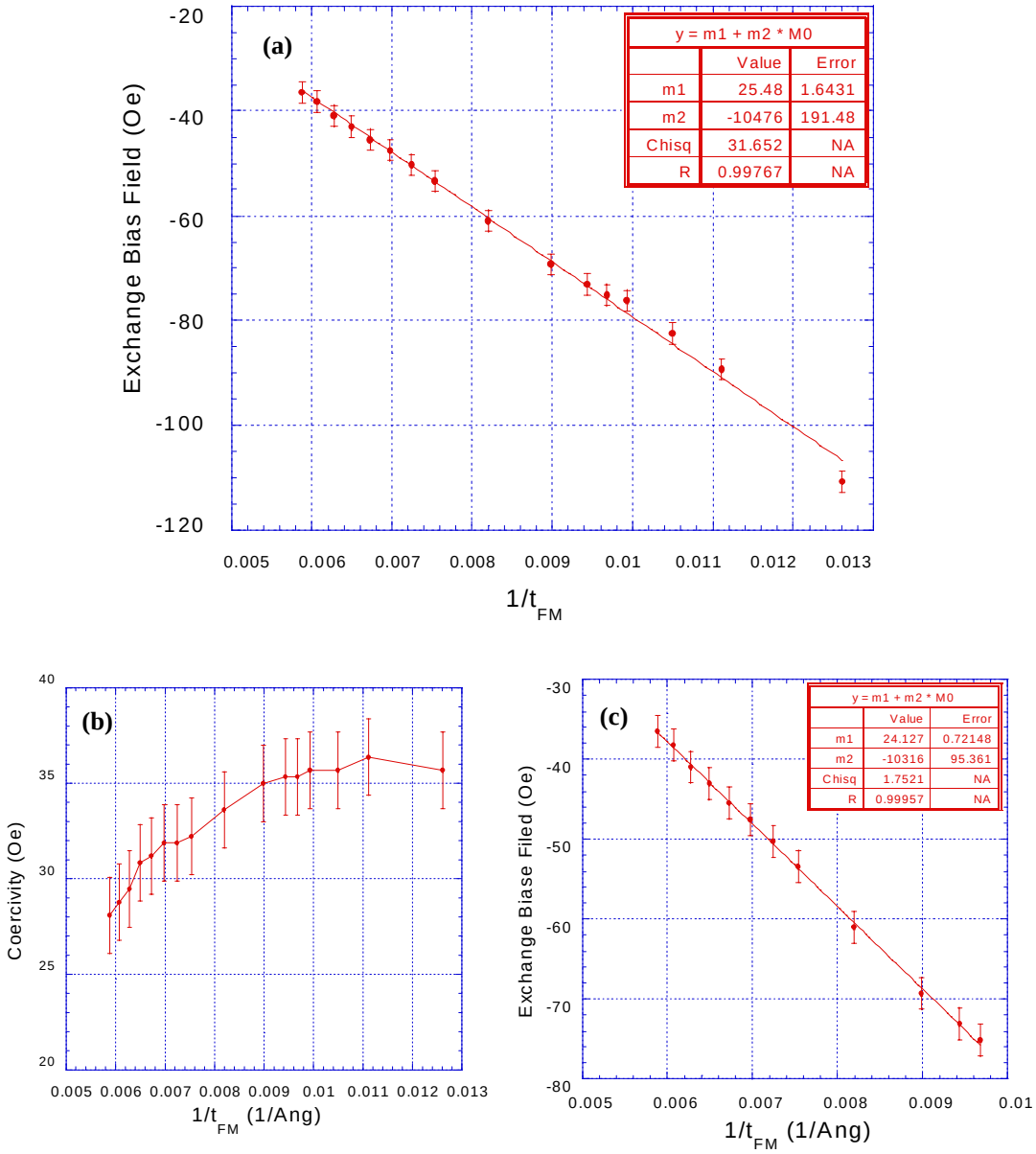

Figure 19: Exchange Biasing and Coercivity of points along the second sample. The exchange biasing data is shown in (a), while in (b) we have plotted the coercivity. The line is a linear fit for the data. The data from the Hall probe measurements was used to correct for the difference in the measured and actual values of the external field at the sample position. In (c), only the data for thicknesses above 100 Å is plotted. The linear fit is much clearer for this data than for that of all thicknesses, suggesting that there is a change in the EB near 100 Å.

Again, the exchange biasing shows a linear dependence on the inverse FM layer thickness. The coercivity increases also, though not linearly. Although the exchange bias

field in this sample does not abruptly disappear at ~ 100 Å thickness as with the old sample, there is an unexpected change in the slope. These results can be clearly seen in Table 1 below.

Second Sample	**SLOPE (in Oe * m)**	**Exchange Bias Energy ΔE (erg/cm^2)**
All data points with corrections	-1.05×10^{-6}	-0.15 +/- 0.003
Corrected data below 100 Å	-1.30×10^{-6}	-0.18 +/- 0.008
Corrected data above 100 Å	-1.03×10^{-6}	-0.15 +/- 0.001

Table 1: Slopes of the fit of exchange biased field with 1/t and calculated exchange biased energy by Equation 29.

Clearly, there is a change around 100Å in the slope of the exchange field. This suggests that perhaps a structural change does occur in the cobalt that can affect the exchange field.

The vertical error in the field takes into account the human error in determining the exchange bias field. The hysteresis loops, once normalized, are used to determine the EB field. There is an uncertainty of 2 Oe in this measurement, which is the error in the EB and coercivity of the measurements.

A systematic error in the x-direction arises from the fact that the initial position of the laser on the sample can only be determined with in an error range of 1 mm, which corresponds to about 5.3 Å of thickness in the sample. This error could result in a shift of the EB, but not a change in the slope. The error in the slope is determined by the 0.01 mm accuracy of the micrometer mount used to translate the sample in the vertical direction. The 0.01 mm corresponds to 0.05 Å difference in thickness, which is an error of 0.01% of the thinnest part of the sample. Theses error bars are too small to be seen in the plots above.

Another factor to take into account is the atomic scale roughness. The surface of the film is not perfectly smooth at the atomic level. However, such fluctuations at the atomic scale are compensated for by the size of the laser spot on the sample. The 1 mm- diameter laser beam

averages over 10^6 atoms at the surface, and thus there is no random scattering of our data points over the various thicknesses.

The slopes given above can be compared with published values for systems using IrMn. While no published research on IrMn/Co has been found, this system's constants can be compared to other similar systems. Since studies of the dependence of the exchange bias field on ferromagnetic thickness (t_{FM}) has shown an inverse dependence on t_{FM}, it is customary to define an interface energy per unit area to compare the strength of the exchange biasing among different materials [3]:

$$\Delta E = M_{FM} t_{FM} H_{EB} \qquad \textbf{(29)}$$

So that the exchange field is given by:

$$H_{EB} = \frac{\Delta E}{M_{FM} t_{FM}} \qquad \textbf{(30)}$$

With M_{FM}=1422 emu/cm^3 for Co [20], equation 30 yields values of ΔE (see Table 1) that fall into the range of those found for IrMn (0.01-0.3 erg/cm^3) [3,22] and in particular the similar system of IrMn/$Co_{90}Fe_{10}$ (ΔE=0.3 erg/cm^3) [22].

According to Malozemoff, the exchange field is given by Equation 25. To test the validity of a model, such as Malozemoff, we need to know the exchange constant and anisotropy of the antiferromagnet. We could not find these numbers for IrMn in the literature, so as an order of magnitude estimate, we take the numbers for FeMn and Co. For FeMn, J ~ 10^{-14} erg, and K = 45 x 10^5 erg/cm^3 [22] and a_0 =3.544 Å for face centered cubic (fcc) Co and a_0 = 2.507 Å for hexagonal (hcp) Co [21]. From Equation 2 we calculate that the slope should be 1.59 x 10^{-5} Oe m for the smooth interface model, and 1.61 x 10^{-6} Oe m for the random roughness model. The

value of the slope calculated from the random roughness model corresponds well with our measured slopes, thus this model seems valid for this system. There has recently been other evidence for the Malozemoff model found in x-ray dichroism experiments of FeMn/Co [23].

VI. **Conclusions and Future work.**

Exchange biasing does occur in IrMn/Co thin films and shows linear dependence on the inverse FM thickness. This is expected from measurements made on other exchange biased systems and from theories of exchange biasing. We also found a thickness dependence in coercivity, as expected. The calculated exchange bias energy was in the range of 0.15 erg/cm^2 to 0.25 erg/cm^2, which is comparable to other measured IrMn systems.

For thicknesses around 100Å, we observed unexpected jumps and changes in the slope of the exchange field as well as the coercivity. The measurements on the third sample confirmed that the exchange field does shift around 100Å. The dependence on inverse thickness is still linear for thicknesses below and above 100Å, with only a change in slope. More data will be taken for thickness less than 100Å to confirm this dependence. Further work is needed to determine why the exchange biasing field shifts around 100 Å. One possibility could be a change in Co structure from fcc to hcp, which could change the exchange biasing either due to a change in lattice parameter in the Co or a change in grain or domain size.

Malozemoff's model gives predictions of the exchange field that correspond well with our experimental data. Future work is needed to explore what mechanisms are responsible for the exchange biasing in this system. For example, if the Mazelmoff model is true, then there should be a dependence of the exchange bias field on the interfacial roughness. To determine if noncollinear spins or uncompensated spins are playing a major role, experiments such as XRMD

(X-ray magnetic dichroism) or neutron scattering can be carried out to probe the spin structure of these samples.

VII. References

[1] W. H. Meiklejohn and C. P. Bean, Phys. Rev., **102**, 1413-1414 (1956).

[2] Miguel Kiwi, J. Magn. Magn. Mater., **234**, 584-595 (2001).

[3] J. Nogués and Ivan K. Schuller, J. Magn. Magn. Mater., **192**, 203-232 (1999).

[4] A. P. Malozemoff, Phys. Rev. B, **35**, 3679-3682, (1987).

[5] Geoff Anderson et al., J. Appl. Phys., **87**, 6989-6991 (2000).

[6] M. N. Rudden and J. Wilson, *Elements of Solid State Physics* (Wiley, New York, 1993), second ed., p. 98.

[7] J. R. Hook, and H. E. Hall, Solid State Physics, (John Wiley and Sons, New York, 1991), Second ed. p. 220.

[8] C. Richard Brundle, Charles A. Evens, Shaun Wilson, *Encyclopedia of Materials Characterization*, (Butterworth-Heinemann, Boston, 1992), p. 723-727.

[9] Paul Lorrain and Dale Corson, Electromagnetic Fileds and Wavesw, (W.H. Freeman and Company, New York, 1972), p 505-511.

[10] J. M. Florczak and E. Dan Dahlberg, J. Appl. Phys. **67**, 7520-7525 (1990).

[11] David S. Kliger, James W. Lewis, and Cora E. Randall, *Polarized Light in Optics and Spectroscopy*, (Academic Press, Inc., Boston, 1990), p. 9-16.

[12] K. H. Bennemann, *Nonlinear Optics*, (Clarendon Press, Oxford, 1998), p. 4-10.

[13] Peter Grunberg, Physics Today, **54**, (2001).

[14] Haiwen Xi and Robert M. White, Phys. Rev. B, **61**, 1318-1323 (2000).

[15] Haiwen Xi and Robert M. White, Phys. Rev. B, **61**, 80-83 (2000).

[16] B. Beschoten, J. Keler, P. Miltenyi, G. Guntherodt. J. Magn. Magn. Mater., (to be published).

[17] Daniele Maurie, Eric Kay, David Scholl, and J. Kent Howard. J. Appl. Phys., **62**, 2929-32 (1987).

[18] Y.J. Tang, B.F.P. Roos, T. Mewes, M. Bauer, So.O. Demokritov, B. Hillebrands, and W. S. Zhan, Mater. Sci. Engin. B, **76**, 59-62 (2000).

[19] A. C. Reilly, W.-C. Chiang,W. Park, S. Y. Hsu, R. Loloee, S. Steenwyk, W.P. Pratt, Jr., and J. Bass, IEEE Transactions on Magnetics, **34**, 939-942 (1998).

[20] B. Cullity, *Introduction to Magnetic Materials* (Addison-Wesley, Reading, MA, 1972). p. 617

[21] R. S. Tebble and D. J. Clark, *Magnetic Materials* (Wiley-Interscience, New York, 1969) p. 50-51.

[22] M. Pakala, Y. Huai, G. Anderson, and L. Miloslavsky, J. Appl. Phys., **87**, 6653-6655 (2000).

[23] W.J. Antel, Jr., F. Perjeru, and G. R. Harp, Phys. Rev. Lett., **83**, 1439-1442 (1999).